SOME OPEN ISSUES IN THE SEISMIC DESIGN OF BRIDGES TO EUROCODE 8-2

Stergios A MITOULIS[1]

Abstract: This paper summarises the ongoing research on the seismic design of isolated and integral bridges at the University of Surrey. The first part of the paper focuses on the tensile stresses of elastomeric bearings that might be developed under seismic excitations, due to the rotations of the pier cap. The problem is described analytically and a multi-level performance criterion is proposed to limit the tensile stresses on the isolators. The second part of the paper sheds light on the response of integral bridges and the interaction with the backfill soil. A method for the estimation of the equivalent damping ratio of short-span integral bridges is presented to enable the seismic design of short period bridges based on Eurocode 8-2. For long-span integral bridges, a novel isolation scheme is proposed for the abutment. The isolator is a compressible inclusion comprises tyre derived aggregates (TDA) and is placed between the abutment and a mechanically stabilised backfill. The analysis of the isolated abutment showed that the compressible inclusion achieves to decouple the response of the bridge from the backfill. The analyses showed that both the pressures on the abutment and the settlements of the backfill soil were significantly reduced under the thermal and the seismic movements of the abutment. Thus, the proposed decoupling of the bridge from the abutment enables designs of long-span integral bridges based on ductility and reduces both construction and maintenance costs.

1 Introduction

Bridges are important infrastructure assets, which are costly to construct and maintain. Integral Abutment Bridges (IABs), which are jointless bridges with piers and/or abutments rigidly connected to the deck, are resilient frame structures that have minimum maintenance requirements, as they do not have bearings or expansion joints. However, integral bridges are expected to respond in an elastic manner (Eurocode 8-2, 2005) when subjected to the design earthquake motion. Hence, the available ductility of the piers is not utilised to reduce the seismic actions. Also, the damping of integral bridges that occurs due to the inelastic behaviour of the backfill (Caltrans, 2013) is not recognised by Eurocode 8-2 as a source of damping. Additionally, in short-span jointless bridges, the kinematic effects in the backfill soil may magnify the displacements of the backfill (Zhang and Makris 2002) and thus increase the displacements of the deck (Inel et al., 2002; Kotsoglou and Pantazopoulou, 2007; Taskari and Sextos 2015). In long-span integral systems, the interaction of the bridge with the backfill soil under serviceability or seismic loads causes significant settlements of the backfill soil (Mitoulis et al., 2014), soil densification and ratcheting flow patterns (England and Tsang, 2001), which increase the soil pressures in the long-term (Arockiasamy M and Sivakumar M 2005). Hence, the condition of the backfill soil deteriorates in time and it requires maintenance and/or replacement that results in bridge closures and costly downtime.

The aforementioned design challenges of integral systems lead to the wide application of seismically isolated bridges. In isolated bridges, the seismic action is being enhanced by bearings, expansion joints and, in some cases, dampers. The structure is required to exhibit zero-damage under the prescribed seismic action and this is the requirement for all the structural components and especially the bearings, on which the overall bridge integrity is relied. However, when the bearings are positively connected to the pier and to the deck, they might be exposed to tensile stresses (Mitoulis, 2014), and this possibility increases when the

[1] Lecturer of Bridge Engineering, University of Surrey, Guildford, s.mitoulis@surrey.ac.uk

bearings are placed eccentrically with respect the axis of the pier, which is common in Southern Europe where precast beams are used for the erection of the deck. Kumar et al. (2014) recognised the potential of bearing uplift and for this reason developed a bearing model that accounts for the tensile non-linear response of elastomeric bearings under extended or beyond design basis shaking. The load deformation of the isolators under pure tensile loads was described before by Constantinou et al. (2007) and Warn (2006). Yang at el. (2010) tested bearings having a shear modulus *G* of 0.55 Mpa under pure tensile loads and identified that the bearing exhibit cavitation (Stanton et al., 2008; Dorfmann[1,2] et al., 2000 and 2003; Yura et al., 2001) when the tensile stresses σ_t exceeded 1-2 Mpa or a strain ε_t of 1%, whilst the bearing uplift potential is evident throughout most bridge design codes (AASHTO, 2012; CalTrans, 1999; EN1998-2, 2005; JRA, 2002).

This paper provides improvements and solutions for the aforementioned challenges of isolated and integral bridges designed to Eurocode 8-2. A criterion that defines three levels of the seismic response of bridge bearings subjected to combined shear, rotation and axial loading is presented to limit the tensile loading of the bearings of isolated bridges. For short-period integral bridges, a methodology for the estimation of the equivalent damping ratio will be described based on a previous research (Mitoulis et al, 2015). The paper concludes with the findings of previous studies on integral abutments that are isolated from the backfill soil by novel compressible inclusions of reused waste materials. It is shown that the proposed design enhances the bridge-backfill interaction under serviceability and seismic displacements of the deck and introduces new cost-effective designs for longer and resilient bridge structures.

2 A stress criterion for mitigating tension in steel-reinforced elastomeric bearings

The recent research on the response of isolated bridges subjected to longitudinal seismic excitations (Mitoulis, 2014) showed that the governing parameters that define the tensile displacements on the bearings are predominantly the eccentricity *e* of the bearing with respect the axis of the pier and the relative rotation of the pier cap and deck, i.e. $r_{pc\text{-}d}= r_{pc}\text{-}r_d$, as shown in Figure 1a and 1b. The following procedure shows how the stresses on the bearing critical edge (see the far edge on Figure 1b) can be calculated based on the combination of: (a) the pure tensile displacement of the bearing $r_{pc\text{-}d} \cdot e$, shown in Figure 1b; (b) the rotation of the bearing $r_{pc\text{-}d}$ shown in Figure 1d and (c) the shearing of the bearing by a displacement of u_x, shown in Figure 1c.

2.1 Tensile stresses on the bearings imposed by the pier cap-deck rotations

The $r_{pc\text{-}d}$ induces a net tensile displacement to the isolators, (Figure 1b) and a net rotation of the bearing, which is equal to $r_{pc\text{-}d}$, as shown in Figure 1d. Hence, the total tensile displacement of the far edge of the bearing $v_{b,seis}^{r_{pc}\text{-}d}$ due to $r_{pc\text{-}d}$ is:

$$v_{b,seis}^{r_{pc\text{-}d}} = (r_{pc} - r_d) \cdot \left(e + \frac{L}{2} \right) \rightarrow v_{b,seis}^{r_{pc}\text{-}d} = r_{pc-d} \cdot \left(e + \frac{L}{2} \right) \quad (1)$$

where *L* in eq.1 is the dimension of the isolator in the longitudinal direction. The axial stiffness K_{vb} of a steel-reinforced bearing is given by Kelly and Konstantinidis (2011):

$$K_{vb} = \frac{E_C \cdot A}{\Sigma t_i} \quad (2)$$

where E_c and *A* are the compression modulus and the area of the isolator respectively and Σ_{ti} is the total thickness of the elastomer. The stress $\sigma_{v,t}$ caused by a net tensile strain of $\varepsilon_{v,t}$ is given by the following equation:

$$\sigma_{v,t}=E_c \cdot \varepsilon_{v,t} \quad (3)$$

For the tensile stress on the far edge of the bearing due to the rotation r_{pc-d} the following procedure was followed. The flexural stiffness K_{rb} of the isolator is:

$$K_{rb} = \frac{E_c I_{eff}}{\Sigma t_i} = 0.329 \cdot \frac{E_C \cdot I}{\Sigma t_i} \tag{4}$$

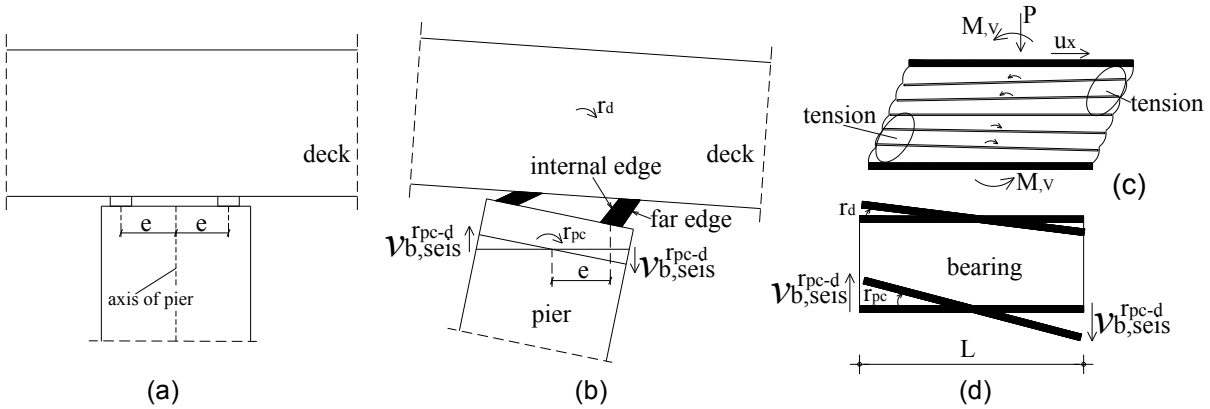

Figure 1. (a) The geometry of the pier cap, (b) the net tensile displacement of the bearings on the right due to the rotation r_{pc-d}, (c) the tensile stresses under shear strains and (d) the rotation of the bearing due to the rotation of the pier cap.

where I and I_{eff} are the moment of inertia of a beam cross-section with the shape of the bearing and the effective moment of inertia correspondingly. The compression modulus E_c' considering incompressibility behavior is:

$$E'_C = 6.073 \cdot G \cdot S^2 \tag{5}$$

where G is the shear modulus of the bearings, S is the bearing shape factor and K is the bulk modulus, which is 2000Mpa (Kelly and Konstantinidis, 2011). It is:

$$E_c = \frac{E'_C \cdot K}{E'_C + K} \tag{6}$$

The stress $\sigma_{v,M}$ at the edge of the isolator due to the rotation of the bearing, which is shown in Fig. 1d, can be estimated based on the following equation:

$$\sigma_{v,M} = \frac{M \cdot (L/2)}{I_{eff}} \tag{7}$$

where M is the bending moment that causes a rotation r_{pc-d} to the bearing, L is the longitudinal dimension of the isolator that is equal to the diameter for a circular bearing, and $y=L/2$ the distance of the edge of the bearing from the neutral axis of the bearing, which remains elastic and is symmetric. The strain $\varepsilon_{v,M}$ of the edge of the bearing due to the rotation r_{pc-d} is:

$$\varepsilon_{v,M} = \frac{r_{pc-d} \cdot (L/2)}{\Sigma t_i} \tag{8}$$

which yields:

$$r_{pc-d} = \frac{\varepsilon_{v,M} \cdot \Sigma t_i}{(L/2)} = \frac{2 \cdot \varepsilon_{v,M} \cdot \Sigma t_i}{L} \tag{9}$$

Also, the bending moment *M* of the isolator is:

$$M = K_{rb} \cdot r_{pc-d} \tag{10}$$

Hence, taking into account equation 7 it is:

$$\sigma_{v,M} = \frac{K_{rb} \cdot r_{pc-d} \cdot (L/2)}{I_{eff}} \Rightarrow \sigma_{v,M} = \frac{K_{rb} \cdot r_{pc-d} \cdot L}{2 \cdot I_{eff}} \tag{11}$$

2.2 Tensile stresses on the bearings due to second order effects

The bending moment due to the shear strain $M_{,V}$, shown in Fig. 1c, also causes tensile stresses to the bearing. The bending moment is:

$$M_{,V} = \frac{P \cdot u_x}{2} \tag{12}$$

where *P* is the vertical load acting on the bearing when the bearing is sheared by a displacement of u_x, as shown in Figure 1c. Hence, the tensile stress of the far edge of the bearing due to $M_{,V}$ is:

$$\sigma_{v,Mv} = \frac{M_{,V} \cdot (L/2)}{I_{eff}} \rightarrow \sigma_{v,Mv} = \frac{-P \cdot u_x \cdot L}{4 \cdot I_{eff}} \tag{13}$$

Notice that *P* is typically a compressive load (i.e. *P<0*) that creates tensile stresses, i.e. $\sigma_{v,Mv} \geq 0$.

2.3 Total tensile stresses on the bearings & proposed performance criterion

The maximum strain of the far edge of the bearing $\varepsilon_{b,ULS}^{max}$ is given by eq. 14:

$$\varepsilon_{b,ULS}^{max} = \varepsilon_{v,t} + \varepsilon_{v,M} + \varepsilon_{v,Mv} + \varepsilon_{b,SLS} \tag{14}$$

where $\varepsilon_{b,SLS}$ is the compressive strain of the bearing due to the self-weight of the deck plus a percentage of the variable loads, i.e. vertical load on the bearing at the onset of the seismic event and $\varepsilon_{v,Mv}$ is the tensile strain due to the $M_{,V}$ Hence, the maximum stress of the far edge of the bearing is:

$$\sigma_{b,ULS}^{max} = \sigma_{v,t} + \sigma_{v,M} + \sigma_{v,Mv} + \sigma_{b,SLS} \leq \sigma_b^{all} = (2 \sim 3) \cdot G \tag{15}$$

where $\sigma_{b,ULS}^{max}$ and $\sigma_{b,SLS}$ are the maximum tensile stress of the bearing during the seismic event (ULS) and the stress of the bearing that corresponds to the $\varepsilon_{b,SLS}$ respectively. Where, σ_b^{all} is the allowable tensile stress of the bearing. The above inequality assumes that the maximum tensile stress that will be induced on the isolator will be smaller than σ_b^{all} *=(2~3)□G*. Taking into account eq. 3, 11 and 13 eq. 15 yields:

$$\sigma_{b,ULS}^{\max} = \mathrm{E_c} \cdot \varepsilon_{\mathrm{v,t}} + \frac{K_{rb} \cdot r_{pc-d} \cdot L}{2 \cdot I_{eff}} - \frac{P \cdot u_x \cdot L}{4 \cdot I_{eff}} + \sigma_{b,SLS} \leq \sigma_{b,t}^{all} = (2 \sim 3) \cdot G \tag{16}$$

The tensile strain due to the net tensile displacement $r_{pc-d} \cdot e$ is:

$$\varepsilon_{v,t} = \frac{r_{pc-d} \cdot e}{\Sigma t_i} \tag{17}$$

If we substituted $\varepsilon_{v,t}$ of eq. 17 in eq. 16 then we get the maximum allowable stress of the far edge of the bearing as follows:

$$\sigma_{b,ULS}^{max} = E_c \cdot \frac{r_{pc-d} \cdot e}{\Sigma t_i} + \frac{K_{rb} \cdot r_{pc-d} \cdot L}{2 \cdot I_{eff}} - \frac{P \cdot u_x \cdot L}{4 \cdot I_{eff}} + \sigma_{b,SLS} \le \sigma_{b,t}^{all} = (2 \sim 3) \cdot G \tag{18}$$

or

$$r_{pc-d} \le \frac{\sigma_{b,t}^{all} - \sigma_{b,SLS} + \frac{P \cdot u_x \cdot L}{4 \cdot I_{eff}}}{\frac{E_c \cdot e}{\Sigma t_i} + \frac{K_{rb} \cdot L}{2 \cdot I_{eff}}} \tag{19}$$

Inequality 19 describes the limit of the relative pier-deck rotation for which the far edge of the bearing under tension (bearing on the right in Figure 1b) will exhibit a maximum tensile stress of σ_b^{all} *=(2~3)□G*. Notice that force *P* is compressive, i.e. *P<0*, and induces a tensile stress at the far edge of the isolator. Also, notice that $\sigma_{b,t}^{all}$*>0* and $\sigma_{b,SLS}$ *<0*, which means that for the bearing to exhibit a tensile stress during an earthquake equal to, say, $\sigma_{b,ULS}^{\max} = 2$ Mpa and the compressive stress of the bearing during SLS is, say, $\sigma_{b,SLS}$ = - 5 Mpa, the tensile displacements of the bearing due to the rotation of the pier cap and due to the shear displacement u_x should cause stress $\sigma_{b,ULS}^{\max} - \sigma_{b,SLS} = 2 - (-5) = 7Mpa$. If we substituted K_{rb} by eq. 4 in eq. 19 we get:

$$r_{pc-d} \le \frac{\sigma_{b,t}^{all} - \sigma_{b,SLS} + \frac{P \cdot u_x \cdot L}{4 \cdot I_{eff}}}{\frac{E_c \cdot e}{\Sigma t_i} + \frac{E_c \cdot L}{2 \cdot \Sigma t_i}} \tag{20}$$

Or taking into account eq. 5 and 6 we get:

$$r_{pc-d} \le \frac{\sigma_{b,t}^{all} - \sigma_{b,SLS} + \frac{P \cdot u_x \cdot L}{4 \cdot I_{eff}}}{\frac{E_c}{\Sigma t_i} \cdot \left(e + \frac{L}{2}\right)} \Rightarrow r_{pc-d} \le \frac{\sigma_{b,t}^{all} - \sigma_{b,SLS} + \frac{P \cdot u_x \cdot L}{4 \cdot I_{eff}}}{\frac{1}{\Sigma t_i} \cdot \frac{6.073 \cdot G \cdot S^2 \cdot K}{6.073 \cdot G \cdot S^2 + K} \cdot \left(e + \frac{L}{2}\right)} \tag{21}$$

Notice that it should always be *P<0*, i.e. the force on the bearing under the maximum shear displacement u_x should be compressive. If *P>0* the bearing will be under tension and hence equation 13 would give a misleading result. Hence it should be:

$$P = \left(\sigma_{b,SLS} + \sigma_{v,t}\right) \cdot A \le 0 \Rightarrow \sigma_{b,SLS} + r_{pc-d} \cdot \frac{E_c \cdot e}{\Sigma t_i} \le 0 \Rightarrow r_{pc-d} \le -\frac{\sigma_{b,SLS} \cdot \Sigma t_i}{E_c \cdot e} \tag{22}$$

Based on eq. 21 we can define the following criterion that represents the maximum allowable stresses of the bearing during SLS and ULS as follows:

$$\begin{aligned} \sigma_{b,t}^{all} &< 2 \cdot G \quad for \quad SLS \\ 2 \cdot G \le \sigma_{b,t}^{all} &\le 3 \cdot G \quad for \quad ULS \end{aligned} \tag{23}$$

The limits of *2·G* and *3·G* were selected based upon the literature (EN15129, 2009; Gent, 1990), which suggests that steel-reinforced bearings do not exhibit significant cavitation for stresses smaller than *2·G* and this was considered adequate for the SLS design situations. Partial cavitation of the elastomer is acceptable for accidental, i.e. infrequent loads that occurs for stresses *(2~3)·G*. Equation 21 was validated by 3D FE models and it was found that the predicted rotation of the pier cap had a maximum deviation of 6% from the FEM.

3 Seismic design of integral abutment bridges

3.1 Damping of short-span integral bridges

A methodology is described in a recent paper for the estimation of the equivalent viscous damping ratio of short-span bridges (Mitoulis et al., 2015). The methodology enables the design of integral bridges in Europe as it can be used for performing simplified response spectrum analysis and displacement-based designs of integral bridges. The methodology was applied on a typical integral abutment with representative backfill soil properties. Numerical analyses of the coupled abutment-backfill system were performed with the FE code PLAXIS. Subsequently, the concept of equivalent viscous damping that was first proposed by Jacobsen (1930), to approximate the steady forced vibration response of linear single degree of freedom SDOF damped systems, was employed, and the hysteretic damping ratios were estimated based on the derived force-displacement curves of the coupled system.

It was observed that the abutment exhibited different behaviours for the two loading conditions that are illustrated in Figure 2, as the abutment is stiffer when it pushes the backfill soil, whereas it is less stiff, when it moves away from it. Interestingly, the hysteretic damping ratios that were estimated for loading condition 2 were higher than the ones that were estimated for the first loading condition for the same target displacement. Also, it was observed that the equivalent damping ratio that was calculated for the bridge of a period of 0.4 sec was approximately 18%, whilst the equivalent damping ratio was found to be approximately 14% for bridges of a period of 0.8 sec. Notably, the above ratios include a 5% damping in the elastic range.

The analysis of equivalent SDOF bridge models, as shown in Figure 3, showed that the damping is successfully predicted by the proposed method for the long-period -0.8sec-systems, whilst for short-period systems (0.4 sec) the proposed method underestimates the damping ratio. Also, the proposed method was not able to account for the formation of the voids that are developed between the abutment and the backfill soil, which soften the system abutment-backfill and hence lead to larger displacements. Further analysis will be conducted to develop a model for the damping of integral bridges designed to Eurocode 8-2 that will account for the increased damping that occurs within the yielding backfill.

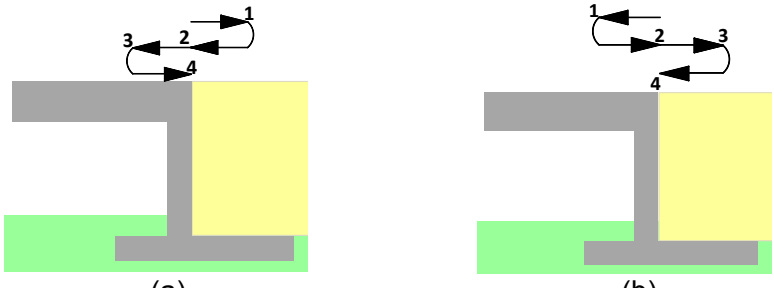

(a) (b)

Figure 2. (a) Loading 1: the abutment first pushes (ps) the backfill soil and (b) loading 2, the abutment first pulls (pl) the backfill soil.

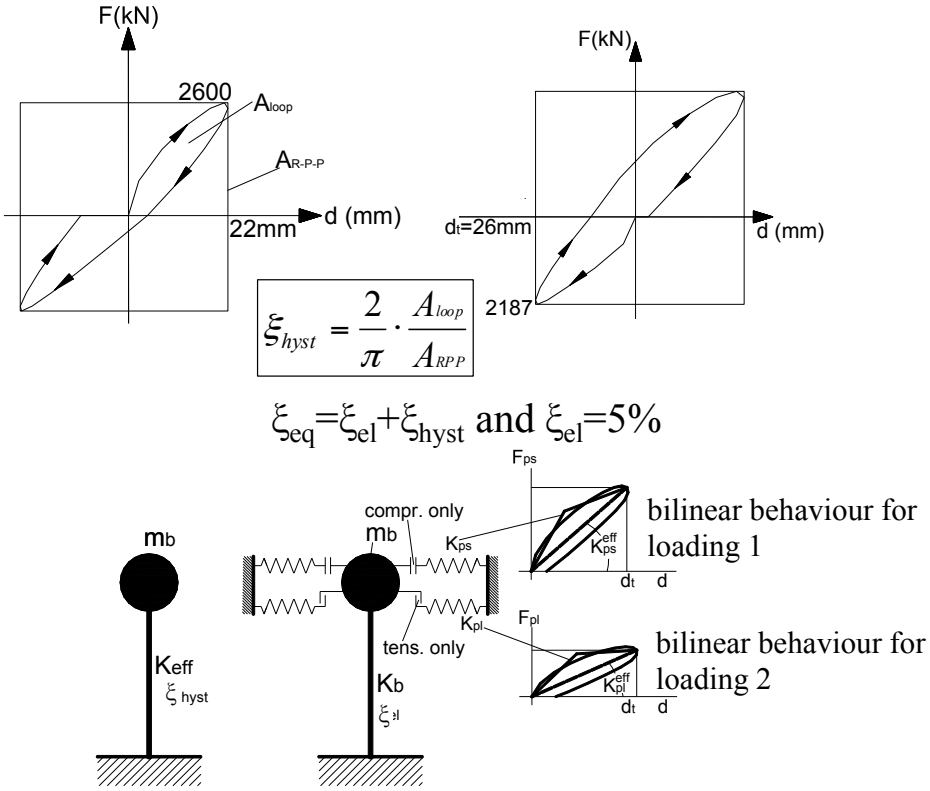

Figure 3: The F-d curves for the bridge (effective period of 0.4sec & target displacement 25mm) and description of the linear and non-linear SDOF models of integral bridges.

3.2 Enhancing the response of long-span integral bridges

An isolation scheme is proposed for integral abutments to mitigate the adverse coupling of the bridge with the backfill soil under serviceability and seismic displacements, as shown in Figure 4. The proposed isolation enables the design of longer maintenance-free bridges. For this purpose, novel compressible inclusions of reused tyre derived aggregates were studied and applied in numerical models of integral abutments with mechanically stabilised backfills. The properties of the compressible inclusions were defined by laboratory tests. An ad-hoc uniaxial test apparatus was produced for this purpose at the Laboratory of Strength of Materials at the University of Surrey. Model compressible inclusions were tested under cyclic compressive strains, which correspond to realistic strains that are imposed to the inclusion by the movements of the integral abutment. The Young's modulus, the permanent deformations and the behaviour of the compressible inclusion was defined under the repetitive loads, strictly for the design purposes of this study. The experimental results were validated with the triaxial tests conducted in Aristotle University of Thessaloniki.

Subsequently, typical integral abutments were modelled and numerical analysis by 2D nonlinear FE model in Plaxis was conducted for bridges with or without compressible inclusions. The validation of the static and dynamic response of the model abutments was presented in a previous paper (Argyroudis et al, 2013). The settlements of the backfill and the soil pressures on the abutment were evaluated for bridges with and without compressible inclusions to assess the efficiency of the compressible inclusion. Figures 5a and b show the settlements and the soil pressures for the conventional and the proposed integral abutment, with the compressible inclusion. The Figures are indicative as they show the results for one seismic motion only, which was scaled to a peak ground acceleration of 0.3g. It is shown that the use of isolators of tyre derived aggregates can enhance the bridge-backfill interaction by reducing significantly the settlements, as shown in Figure 5a, and the pressures on the abutment, as shown in Figure 5b. Therefore, the isolation of the abutment from the backfill

soil is key to the application of long-span integral bridges. Also, it was observed that the bridge, which had its abutments isolated from the backfill soil, exhibited displacements which were significantly larger than the conventional integral bridge. Hence, the available ductility of the piers of integral bridges can be utilised as a means to reduce the seismic actions of this type of bridges, i.e. a behaviour factor larger than one proposed by Eurocode 8-2 can be used.

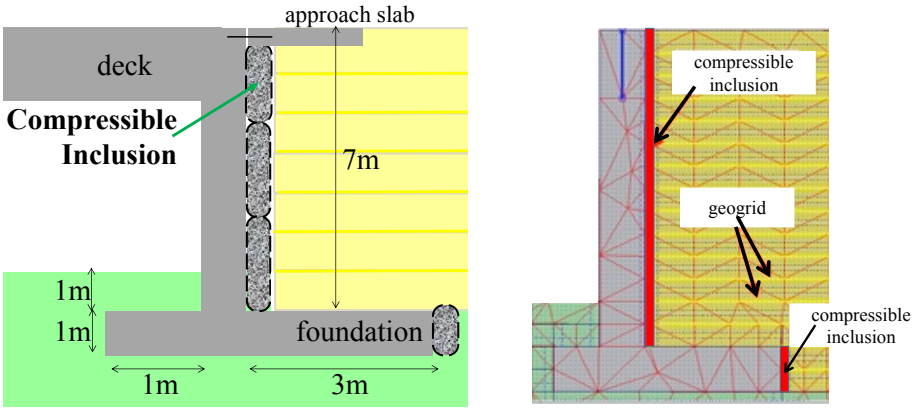

(a) (b)

Figure 4: (a) The isolation of the abutment with compressible inclusions and (b) the 2D FE model that was analysed in PLAXIS.

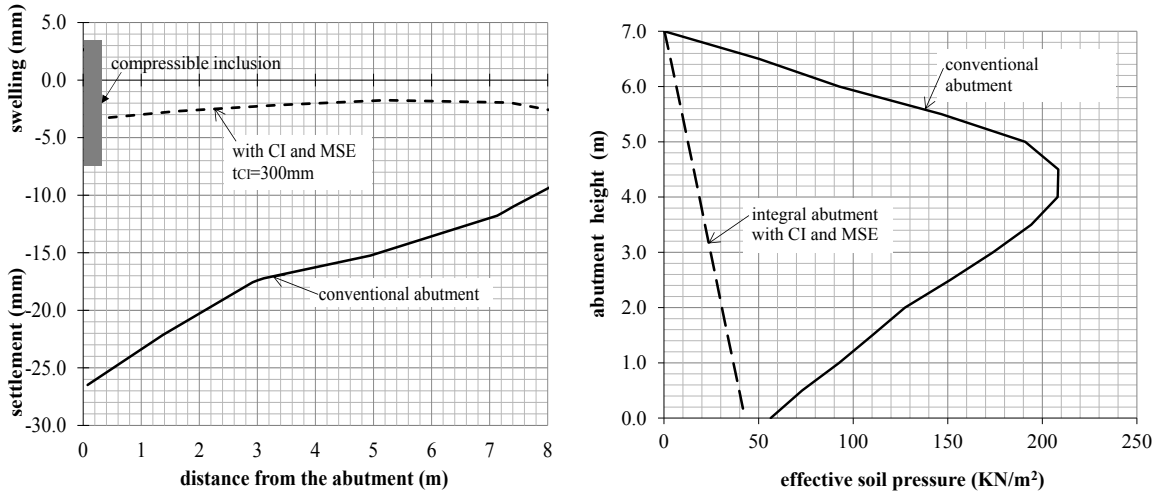

(a) (b)

Figure 5. (a) The swelling and the settlements of the backfill soil for integral abutments with and without compressible inclusions and (b) the soil pressures on the abutment (indicative).

Conclusions

A synopsis of the research that is being conducted at the University of Surrey on earthquake resistant bridges was presented. Open issues on the design of seismically isolated and integral bridges were presented and solutions were proposed. The main outcomes of the research are summarised below:

The design of seismically isolated bridges with bearings eccentrically placed on the pier cap, which is common practice in Southern European countries, is required to account for potential tensile loading in the bearings. A stress-based criterion was described in this paper. The criterion was developed by applying elastic beam theory and defined the maximum tensile stresses at the critical edge of the bearing. The analytical model was validated through a FE model of a single-pier with steel-reinforced bridge bearings. The criterion

suggests three levels of bearing tensile stresses that represent SLS (no cavitation), ULS (potential of cavitation) and extensive cavitation of the elastomer of the isolator. The bounds of the aforementioned stress criterion were decided upon the international literature, the available laboratory tests and the current Eurocode provisions. The proposed criterion can be useful for limiting the rotation of the piers for different bridge types and for bearings placed either concentrically or eccentrically with respect the pier cap. This criterion was found to predict with acceptable accuracy the maximum tensile stress of the critical edge of the bearing.

The seismic response and design of integral abutment bridges to Eurocode 8-2 was discussed for both short- and long-span systems. For the short period integral bridges, the ongoing research on the estimation of the damping ratio of bridges is discussed based upon a previous paper. The studies to date resulted in equivalent damping ratios higher than the ones prescribed by Eurocode 8-2. Further verification of the numerical studies will be conducted with the aim to develop a model for the estimation of the equivalent damping ratio of integral bridges to simplify the analysis and design of this particular type of bridges in Europe.

A novel solution for long-span frame bridges was presented. The experimental and numerical studies conducted in collaboration with Aristotle University of Thessaloniki concluded that the isolation of integral abutments from the backfill soil by means of ad-hoc compressible inclusions, enables the design of longer and ductile integral bridges. Additionally, the isolation of the bridge by means of reused tyre derived aggregates enhances the long-term performance of the system as both the settlements of the backfill and the soil pressures on the abutment are significantly reduced.

REFERENCES

American Association of State Highway and Transportation Officials [AASHTO] (2012) *LRFD bridge design specifications*. 6th ed., with 2013 interim revisions. Washington, DC

Argyroudis SA, Mitoulis SA, Pitilakis KD (2013) Seismic response of bridge abutments on surface foundation subjected to collision forces, COMPDYN 4th International Conference in Computational Methods in Structural Dynamics and Earthquake Engineering, Kos, Greece, 12-14 June 2013.

Arockiasamy M, Sivakumar M (2005) Time-Dependent Behavior of Continuous Composite Integral Abutment Bridges, *Pract. Period. Struct. Des. Constr.,* 10(3), 161–170

California Department of Transportation [CalTrans] (1999) *Bridge memo to designers (20-1) – Seismic design methodology*. Sacramento, CA.

California Department of Transportation [CalTrans] (2013) *Seismic design criteria*, Version 1.7

Constantinou MC, Whittaker A S, Kalpakidis Y, Fenz DM, Warn GP (2007) Performance of Seismic Isolation Hardware Under Service and Seismic Loading, *Report 07-0012, MCEER*, Buffalo, New York

Dorfmann A, Burtscher SL (2000) Aspects of cavitation damage in seismic bearings, *Journal of Structural Engineering*, 126:573-579.

Dorfmann A (2003) Stress softening of elastomers in hydrostatic tension, *Acta Mechanica*, DOI 10.1007/s00707-003-0034-5

EN 1337-3 (2005) *Structural bearings – Part 3: Elastomeric bearings*.

EN 15129:2009. Anti-seismic devices, BSI British Standards.

EN 1998-2 (2005) Eurocode 8: *Design of structures for earthquake resistance, Part 2: Bridges*

England GL, Tsang NC (2001) *Towards the design of soil loading for integral bridges-experimental evaluation*, Department of Civil and Environmental Engineering, Imperial College, London

Gent A (1990) Cavitation in rubber: a cautionary tale. *Rubber Chemistry and Technology*; 63:49.

Iemura H, Taghikhany T, Takahashi Y, Jain S (2005) Effect of variation of normal force on seismic performance of resilient sliding isolation systems in highway bridges, *Earthquake Engineering and Structural Dynamics*, 34: 1777-1797

Inel, M. and Aschheim, M. (2004) Seismic Design of Columns of Short Bridges Accounting for Embankment Flexibility, *Journal of Structural Engineering*, 130(10), 1515–1528.

Jacobsen LS (1930) Steady forced vibrations as influenced by damping. *Transactions of the American Society of Mechanical Engineers*, 52, 169-181

Japan Road Association (1997) *Manual for seismic design of highway bridges*, Tokyo.

Kelly JM, Konstantinidis DA (2011) *Mechanics of Rubber Bearings for Seismic and Vibration Isolation*, JohnWiley & Sons Ltd

Kotsoglou A, Pantazopoulou S (2007) Bridge–embankment interaction under transverse ground excitation, *Earthquake Engineering & Structural Dynamics*, 36(12), 1719–1740

Kumar M, Whittaker AS, Constantinou MC (2014) An advanced numerical model of elastomeric seismic isolation bearings, *Earthquake Engineering and Structural Dynamics*, 43:1955-1974

Mitoulis SA, Muhr A, Ahmadi H (2014) *Uplift of elastomeric bearings in isolated bridges-A possible mechanism: Effects and remediation*, Proceedings of the 15th European conference on earthquake engineering, Istanbul 2014

Mitoulis SA, Argyroudis S, Kowalsky M (2015) Evaluation of the stiffness and damping of abutments to extend DDBD to the design of integral bridges, COMPDYN 2015, 5th ECCOMAS Thematic Conference on Computational Methods in Structural Dynamics and Earthquake Engineering, Crete

Mitoulis (2014) Uplift of elastomeric bearings in isolated bridges subjected to longitudinal seismic excitations, *Structure and Infrastructure Engineering*, DOI: 10.1080/15732479.2014.983527

Mitoulis SA, Argyroudis S, Pitilakis KD (2014) Green rubberised backfills to enhance the longevity of integral abutment bridges, *15th European conference on earthquake engineering*, Istanbul 2014

Stanton JF, Roeder CW, Mackenzie-Helnwein P, White C, Kuester C and Craig B (2008) Rotation limits for elastomeric bearing, *National Cooperative Highway Research Program Report No. 596,* Trans. Research Board, Washington, D.C., National Academy Press

Taskari O, Sextos A (2015) Probabilistic assessment of abutment-embankment stiffness and implications in the predicted performance of short bridges, Journal of Earthquake Engineering, doi:10.1080/13632469.2015.1009586

Warn GP (2006) *The coupled horizontal-vertical response of elastomeric and lead-rubber seismic isolation bearings*, PhD Dissertation, University at Buffalo

Yang QR, Liu WG, He WF, Feng DM (2010) Tensile stiffness and deformation model of rubber isolators in tension and tension-shear states, *Journal of Engineering Mechanics*, 136:429-437.

Yura J, Kumar A, Yakut A, Topkaya C, Collingwood E (2001) Elastomeric bridge bearings: Recommended test methods, *National Cooperative Highway Research Program Report No. 449*, Trans. Research Board, Washington, D.C., National Academy Press

Zhang J, Makris N (2002) Kinematic response functions and dynamic stiffnesses of bridge embankments. *Earthquake Engineering Structural Dynamics,* 31:1933–1966